Spatially-Modulated Radar Waveforms Inspired by Fixational Eye Movement

Shannon D. Blunt[1], Patrick McCormick[1], Thomas Higgins[2], and Muralidhar Rangaswamy[3]
[1]Radar Systems Lab, University of Kansas, Lawrence, KS
[2]Radar Division, Naval Research Laboratory, Washington, DC
[3]Sensors Directorate, Air Force Research Laboratory, Dayton, OH

***Abstract* – We consider a class of MIMO radar emissions in which a coherent spatial beam is formed while the direction is modulated during the pulse width. This type of spatial modulation has a direct analog to the rapid, small movements of the human eye during fixation (staring) to enhance contrast and sensitivity to fine detail. To replicate this passive sensing capability of the eye for the active sensing modality of radar we leverage and expand the continuous phase modulation (CPM) framework for code-to-waveform implementation and thereby realize a physical delay-angle coupled emission. Through analysis of a defined angle-delay ambiguity function for specific waveform/spatial modulation examples it is shown that enhanced discrimination is enabled at the cost of some SNR loss, which may be an acceptable tradeoff for some applications.**

I. Introduction

Traditionally, a radar system emits a waveform-modulated pulse in a given spatial direction. With the advent of electronically steered arrays this emission is achieved by applying a fixed inter-element phase shift across the antenna array, with an otherwise identical waveform being generated by each antenna element. The subsequent received echoes are characterized by the same waveform response regardless of spatial direction. However, the multiple transmit channels of the array represent a source of design freedom that may be exploited to develop new sensing structures that are collectively ascribed the moniker of MIMO, which includes the extremes from standard beamforming to completely independent waveforms on each array element and all variations in between. The majority of work in the literature has focused on the theoretically optimal design of MIMO waveforms and receiver processing under various statistical assumptions ([1] and references therein). In contrast, and complementary to that work, we consider the physical instantiation of a class of correlated MIMO emissions that can be readily implemented in hardware and subsequently evaluate performance for a few exemplary cases.

The notion of transmitting different, albeit correlated, waveforms simultaneously from the elements on an array has been proposed [2-5] as a method to broaden the transmit beamwidth (i.e. beam-spoiling) for the purpose of achieving, for example, simultaneous multi-mode radar. Likewise, changing the beampattern in a pulse-to-pulse (*inter*-pulse) manner has been proposed for subsequent adaptive processing (e.g. [6]) and even forms the basis of an early form of target angle estimation related to monopulse known as sequential lobing [7], though the latter is an inefficient use of radar resources and is susceptible to inter-pulse target amplitude fluctuations. Alternatively, we consider the case in which the pulsed radar emission possesses both a temporal modulation (the waveform) and an *intra*-pulse spatial modulation that is a form of fast-time time-division beamforming, an example of which is the frequency-diverse array concept [3-5].

There is an interesting biological analog to this fast-time direction changing found in the visual system of humans and animals possessing fovea in which the particular direction of attention is spatially modulated, in a seemingly random manner (Fig. 1), via slow eye movements known as *drift* and rapid eye movements known as *microsaccades* [8,9]. While the purpose of these *fixational eye movements* has long been debated and remains an open research topic in the biological community, the current consensus is that these spatial perturbations improve visual acuity because the associated transients enhance contrast and sensitivity as well as aid in the resolving of spatial ambiguities. Furthermore, there is evidence [10] that these eye movements adapt according to environmental conditions (e.g. amount of lighting) and the active attention of the observer thus suggesting a linkage between the physical actuation of the sensor and cognition, which for the extension here to active sensing thus implies an application within the context of cognitive radar [11].

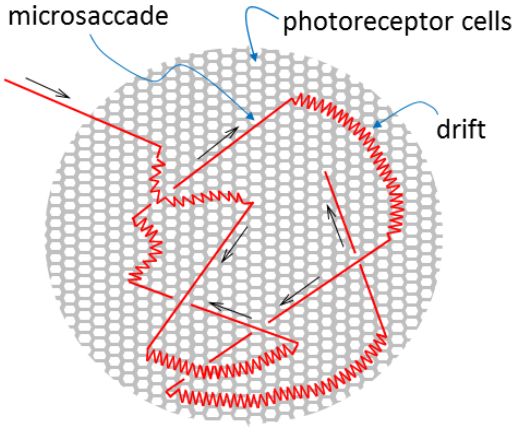

Figure 1. Example of eye movement during fixation

In light of this visual/neurological antecedent we consider the concept of fast-time spatial modulation within the radar emission by employing an inter-element phase shift across the array that varies during the pulsewidth. This emission strategy forms a subset of the general class of MIMO radar transmit

This work was supported in part by the Air Force Office of Scientific Research and the Office of Naval Research base funding program.

schemes. Here, an approach denoted as the waveform diverse array (WDA) is used to allow for arbitrary waveform selection and provide control over the fast-time-dependent spatial beampattern. The characteristics of the WDA approach are assessed relative to the traditional beamformed emission by examining the time-varying beampattern, the aggregate beampattern over the pulsewidth, and an angle-delay ambiguity function. Further, attention is focused on the performance resulting from matched filtering upon receive to ascertain the practical performance one might achieve by implementation of this physical angle-delay coupled emission scheme for existing hardware and computational capabilities.

II. Waveform-Diverse Array

The similarity to fixational eye movement in biology clearly suggests the use of a two-dimensional array. However, while the WDA concept is applicable to any array geometry, for the sake of illustration we shall focus attention on the uniform linear array (ULA). For a ULA with element spacing d the spatial angle θ is here defined relative to array boresight (where $\theta = 0°$). It is assumed that emitted/received signals satisfy the array narrowband assumption so the electrical phase angle is $2\pi d \sin(\theta)/\lambda$, with λ the wavelength associated with the carrier frequency.

A. WDA Definition

The waveform diverse array (WDA) concept presumes a means of independent waveform generation behind each element of the antenna array. To link the phase modulation of the waveform with the element-wise spatial modulation we leverage the continuous phase modulation (CPM) framework [12-14] that generates polyphase-coded FM (PCFM) waveforms that are both constant modulus and continuous (thus differentiable with good spectral containment).

First, given a radar code with $N + 1$ chip phase values denoted as $\phi_0, \phi_1, \cdots, \phi_N$, a train of N impulses with time separation T_p are formed such that the total pulsewidth is $T = NT_p$. The n^{th} impulse is weighted by α_n, the phase change between successive chips of the polyphase code determined by

$$\alpha_n = \begin{cases} \tilde{\alpha}_n & \text{if } |\tilde{\alpha}_n| \le \pi \\ \tilde{\alpha}_n - 2\pi \operatorname{sgn}(\tilde{\alpha}_n) & \text{if } |\tilde{\alpha}_n| > \pi \end{cases}, \quad (1)$$

where

$$\tilde{\alpha}_n = \phi_n - \phi_{n-1} \quad \text{for} \quad n = 1, \cdots, N, \quad (2)$$

sgn(•) is the signum operation, and ϕ_n is the n^{th} chip phase value in the polyphase code. The shaping filter $g(t)$ may, for example, be rectangular (RECT) or raised cosine (RC) with the requirements 1) that it integrates to unity over the real line; and 2) that it has a time support on $[0, T_p]$. The continuous PCFM waveform can thus be expressed as

$$s(t; \mathbf{x}_w) = \exp\left\{ j \left(\int_0^t g(\tau) * \left[\sum_{n=1}^{N} \alpha_n \, \delta\left(\tau - (n-1)T_p\right) \right] d\tau + \phi_0 \right) \right\}, \quad (3)$$

where $*$ denotes convolution, ϕ_0 is the initial phase value in the code, and the sequence of phase changes are collected into the vector $\mathbf{x}_w = [\alpha_1 \ \alpha_2 \ \cdots \ \alpha_N]^T$ which parameterizes the complex baseband waveform.

This code-to-waveform implementation can likewise be extended to parameterize in a physical manner the fast-time modulation of relative phase across the antenna array to facilitate spatial modulation over the pulsewidth. Here a *spatial modulation code* comprised of $N + 1$ values denoted as $\Delta_0, \Delta_1, \cdots, \Delta_N$, is defined as a sequence of spatial angle offsets relative to some center direction θ_C. The subsequent spatial phase-change sequence in terms of electrical angle is thus

$$\varepsilon_n = \frac{2\pi d}{\lambda}\left(\sin(\theta_C + \Delta_n) - \sin(\theta_C + \Delta_{n-1}) \right) \quad (4)$$

for $n = 1, 2, \cdots, N$, noting that the values Δ_n can be positive or negative and are small enough (when combined with θ_C) to avoid spatial "wrap around". Echoing the structure of (3), the spatial phase modulation as a function of continuous time is

$$b(t; \mathbf{x}_s) = \exp\left\{ -j \left(\int_0^t g(\tau) * \left[\sum_{n=1}^{N} \varepsilon_n \, \delta\left(\tau - (n-1)T_p\right) \right] d\tau + \bar{\Delta}_0 \right) \right\} \quad (5)$$

where the sequence of spatial phase changes are collected into the vector $\mathbf{x}_s = [\varepsilon_1 \ \varepsilon_2 \ \cdots \ \varepsilon_N]^T$ and the initial electrical angle is

$$\bar{\Delta}_0 = \frac{2\pi d}{\lambda} \sin(\theta_C + \Delta_0). \quad (6)$$

The negative sign prior to the j in (5), relative to (3), reflects the phase delay compensation for transmit beamforming.

Given M antenna elements, indexed as $m = -(M-1)/2, -(M-1)/2 + 1, \cdots, +(M-1)/2$ so that 0 is located at the center of the array, the emission from the m^{th} antenna element is defined as

$$s_m(t, \theta_C; \mathbf{x}_w, \mathbf{x}_s) = \frac{1}{\sqrt{T}} s(t; \mathbf{x}_w) \, b^m(t; \mathbf{x}_s). \quad (7)$$

The normalization in (7) provides unit transmit energy per antenna element. The Vandermonde form $(\bullet)^m$ in (7) yields

$$b^m(t; \mathbf{x}_s) = \exp\left\{ -jm \left(\int_0^t g(\tau) * \left[\sum_{n=1}^{N} \varepsilon_n \, \delta\left(\tau - (n-1)T_p\right) \right] d\tau + \bar{\Delta}_0 \right) \right\}. \quad (8)$$

In the case of no spatial modulation, $\Delta_0 = \Delta_1 = \cdots \Delta_N = 0$ results so that, from (4), (6) and (8), a stationary beam is formed in the direction of spatial angle θ_C.

The combined waveform/spatial modulation in (7) remains a form of frequency modulation (FM) that, as demonstrated by the widespread use of CPM for aeronautical telemetry, deep-space communications, and the Bluetooth™ wireless standard, can be physically generated without the need for an arbitrary waveform generator. As such, this emission scheme is both physically realizable and economically feasible.

B. WDA Beampattern and Ambiguity Analysis

The WDA emission can be assessed by examining the time-varying beampattern, aggregate beampattern, and the angle-delay ambiguity function. The definitions of these metrics are based on the normalized baseband representation of the composite far-field emission as a function of time t and spatial angle θ given by

$$g(t,\theta,\theta_C) = \frac{1}{M}\sum_{m=-(M-1)/2}^{(M-1)/2} s_m(t,\theta_C)\, e^{jm\,2\pi d\sin(\theta)/\lambda}, \qquad (9)$$

where $s_m(t, \theta_C)$ is taken from (7) and the exponential term is the delay imparted due to path length differences as a function of θ. The dependence on the waveform code $\mathbf{x}_w$ and spatial code $\mathbf{x}_s$ have been suppressed for brevity. If the set of M waveforms $s_m(t, \theta_C)$ are identical aside from a scalar phase shift (i.e. no spatial modulation) then the emission in (9) is just the original waveform $s(t)$ beamformed in the direction θ_C. In other words, the temporal modulation is decoupled from the spatial angle. Otherwise, however, different waveforms will be observed at different spatial angles θ in the far-field.

Using (9), the instantaneous spatial features can be examined using the time-varying beampattern (TVBP)

$$B_{TV}(t,\theta,\theta_C) = g(t,\theta,\theta_C)\, g^*(t,\theta,\theta_C) \qquad (10)$$

for $0 \le t \le T$, where $(\bullet)^*$ denotes complex conjugation. Integrating (10) over the pulse width yields the aggregate beampattern

$$B(\theta,\theta_C) = \frac{1}{T}\int_0^T g(t,\theta,\theta_C)\, g^*(t,\theta,\theta_C)\, dt\,. \qquad (11)$$

As discussed above, if no spatial modulation is present the product in (11) is constant over the pulse width so $B(\theta,\theta_C)$ yields the usual *array factor* beampattern [15] steered to θ_C.

Also using (9), an angle-delay ambiguity function (ADAF) can be constructed as

$$A(\tau,\theta,\beta,\theta_C) = \left| \frac{\int_0^T \left[\sum_{m=-(M-1)/2}^{(M-1)/2} g(t,\theta,\theta_C) e^{jm\bar{\theta}}\, g^*(t-\tau,\beta,\theta_C) e^{-jm\bar{\beta}}\right] dt}{M\left[\int_0^T g(t,\beta,\theta_C)\, g^*(t,\beta,\theta_C)\, dt\right]^{1/2}} \right|^2 \qquad (12)$$

where τ is the relative delay of the incident signal, the electrical angle of a signal arriving from spatial angle θ is

$$\bar{\theta} = \frac{2\pi d}{\lambda}\sin(\theta)\,, \qquad (13)$$

and the electrical angle corresponding to the receive filter tuned to spatial angle β is

$$\bar{\beta} = \frac{2\pi d}{\lambda}\sin(\beta)\,. \qquad (14)$$

In (12), the factor M normalizes the receive beamforming and the integral in the denominator normalizes the matched filter $g^*(t,\beta,\theta_C)$ to unity gain. Due to the normalization factors in (7), (9), and (12), the standard beamforming (no spatial modulation) response of (12) at $\tau = 0$ and $\beta = \theta = \theta_C$ achieves the maximum value of 0 dB. Thus the "beam smearing" loss of spatial modulation can be directly determined. Also, while not considered here, Doppler can be readily incorporated into (12) for an angle-delay-Doppler ambiguity function. Finally, as long as the array narrowband assumption holds the emission and subsequent analysis framework of (7), (9), and (12) can be easily modified for arbitrary array structures.

III. Spatially-Modulated Emission Examples

Consider a ULA comprised of $M = 30$ elements, a linear FM chirp implemented using the CPM framework of (1)-(3) for $N = 200$ (which approximates the time-bandwidth product), and boresight center direction ($\theta_C = 0°$). For the time interval of a single pulse (vertical axis), Figure 2 illustrates the time-varying beampattern (horizontal axis) defined in (10) for the examples of Case 1: standard beamforming (no spatial modulation), Case 2: null-to-null linear spatial modulation, Case 3: double null-to-null linear spatial modulation, and Case 4: null-to-null sinusoidal spatial modulation. The first three cases can be viewed as pulsed (and thus truncated) versions of the frequency-diverse array concept [3-5]. These examples are used to illustrate some of the characteristics of spatial modulation. Obviously there are myriad different spatial modulation codes that could be used to produce different time-varying beampatterns over the pulsewidth.

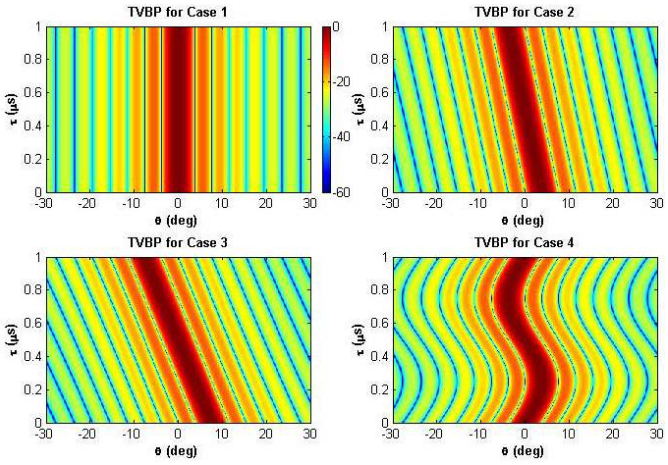

Figure 2. Time-varying beampattern over the pulsewidth via (10)

For these four example cases, Fig. 3 illustrates the aggregate beampatterns using (11), in which it is observed that the spatial modulation incurs a loss relative to the standard beamforming of Case 1 as a result of spreading the transmit energy in space. Further, one might surmise from Fig. 3 that spatial modulation leads to a degradation in spatial resolution. However, this conclusion would be incorrect as the aggregate beampattern of (11) does not account for the decorrelation of the far-field emission as a function of spatial angle (which is different from the use of uncorrelated waveforms on different

antenna elements). To determine the spatial resolution one must examine the angle-delay ambiguity function of (12).

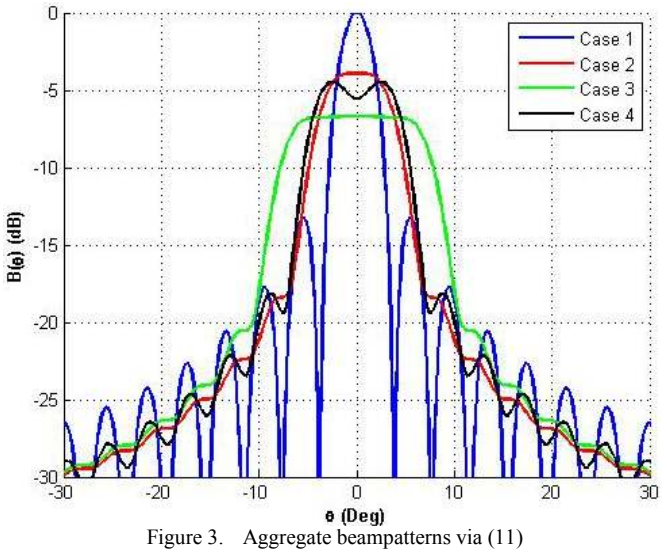

Figure 3. Aggregate beampatterns via (11)

It is instructive to examine some of the various cuts of the ambiguity function defined in (12) for these emission scenarios. Figure 4 depicts the delay matched point ($\tau = 0$) cut of the angle-delay ambiguity function for each of the four cases where the horizontal axis is the angle β of the receive filter and the vertical axis is the incident angle θ. The responses in Fig. 4 illustrate the impact of temporal cross-correlation between the different angle-dependent emissions. It is interesting to note that, outside of the elongated mainlobe (along the $\theta = \beta$ axis), the sidelobes of the spatial modulation cases (2-4) appear to be somewhat lower than that exhibited by standard beamforming of Case 1.

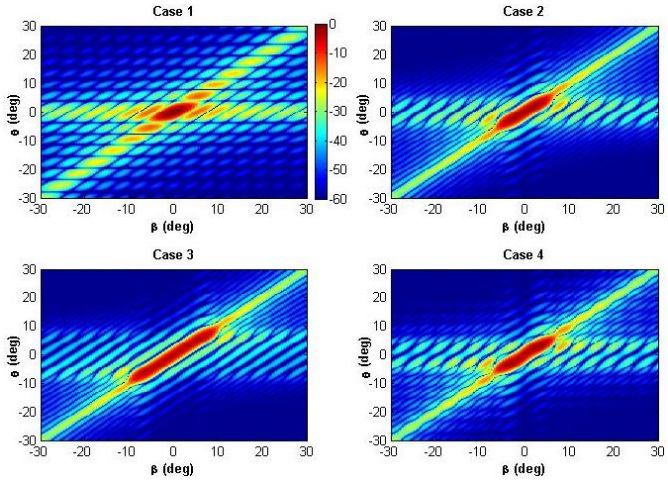

Figure 4. $\tau = 0$ cut of angle-delay ambiguity function from (12)

Taking the $\theta = 0$ cut of the responses in Fig. 4 and peak-normalizing for easy comparison yields the results shown in Figs. 5 and 6 (the latter is a close-up of the mainbeam). It is observed that the spatial modulation cases realize both lower spatial sidelobes (relative to the mainlobe) and enhanced spatial resolution, the latter by 23%, 27%, and 30% for Cases 2, 3, and 4, respectively when measured 3 dB from the peak and in comparison to standard beamforming (Case 1).

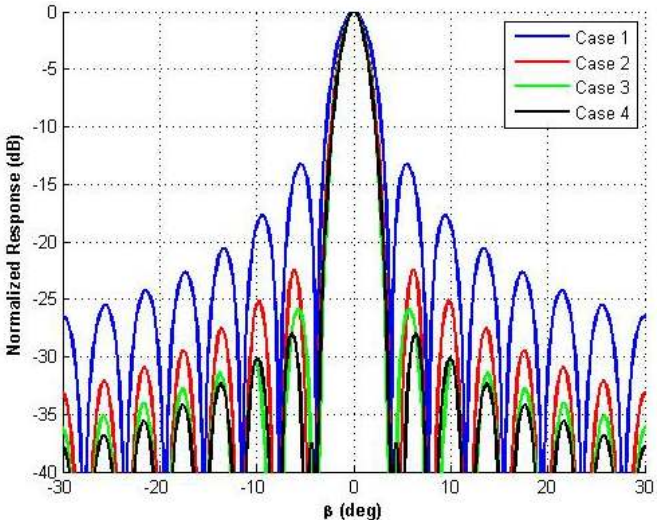

Figure 5. $\tau = 0$, $\theta = 0$ cut of peak-normalized ADAF from (12)

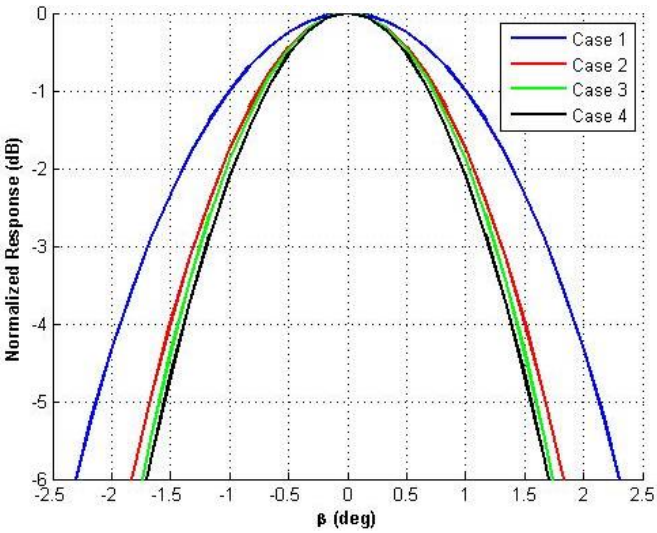

Figure 6. $\tau = 0$, $\theta = 0$ cut of peak-normalized ADAF (mainbeam)

Returning to the original angle-delay ambiguity function of (12), now consider the $\theta = 0$ cut with arbitrary τ and β. Figure 7 depicts this aspect of the ambiguity function for the four cases where the sidelobes in the delay dimension (vertical axis) are noticeably reduced for the linear spatial modulation cases (2 and 3). For a closer inspection consider the $\beta = 0$ cut as before where it is observed (Fig. 8) that the range sidelobes are substantially reduced at the cost of some degradation in range resolution. In contrast, the sinusoidal spatial modulation (Case 4), which was found to provide marginally the best spatial resolution and sidelobes (of these cases) in Figs. 4 and 5, exhibits quite poor performance in the delay domain with no clear mainlobe and very slow sidelobe roll-off.

The linear spatial modulation results in the delay domain (Fig. 8) can be likened to an amplitude tapering of an LFM waveform, albeit one that is occurring in the far-field due to

fast-time-dependent beamforming as opposed to within the transmitter (where the latter is well known to incur a power efficiency loss due to operation of the power amplifier in the linear regime). However, it is important to note that here the range resolution degradation is linked to the enhanced resolution in the spatial domain. In other words, one can infer an attendant coupling that may enable some degree of trade-off between range and spatial resolution which necessitates examination of how one may go about jointly optimizing these coupled physical emissions (e.g. generalization of [16,17]).

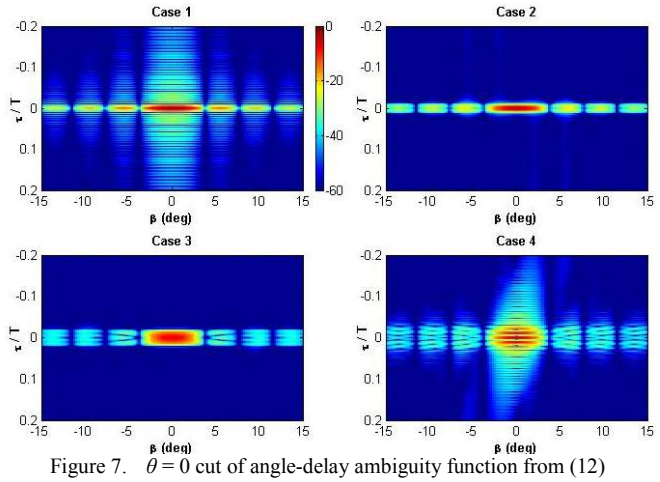

Figure 7. $\theta = 0$ cut of angle-delay ambiguity function from (12)

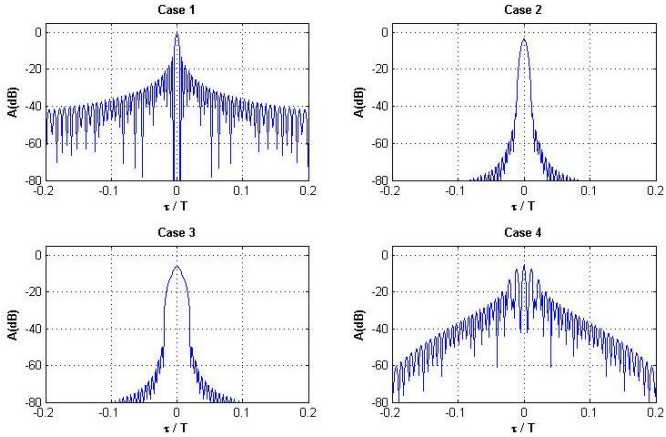

Figure 8. $\theta = 0, \beta = 0$ cut of ambiguity function in (12)

Finally, consider a example scenario in which five targets exist in a cross pattern, with three of the targets occupying the same range cell (index 200) at spatial angles $-4°$, $0°$, and $+4°$, and two more targets reside at spatial angle $0°$ at range indices 192 and 208. The same four illumination schemes are used with the responses sampled in range at a rate of 3 samples / "transition interval" according to the continuous PCFM waveform structure defined in [14].

Figures 9-12 depict the delay-angle output generated by normalized beamforming across receive angle β and associated unity-gain-normalized pulse compression matched filtering as employed to define the angle-delay ambiguty function of (12). The standard beamforming result in Fig. 9 clearly illustrates the range-delimited targets. However, the angle-separated targets at range index 200 are not visible.

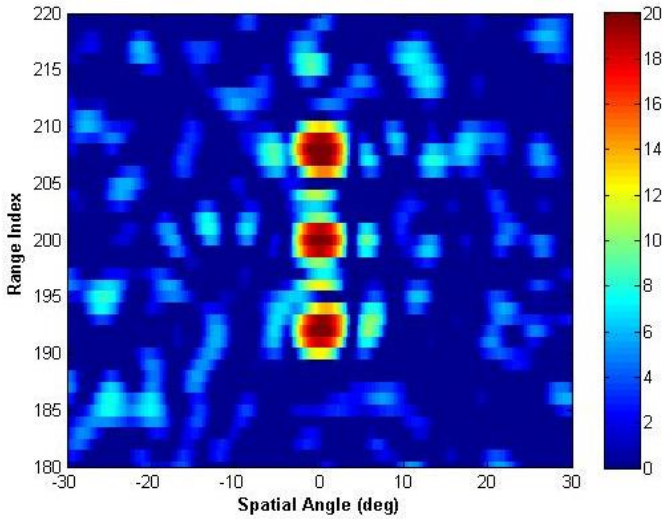

Figure 9. Five-target scenario for Case 1) standard beamforming

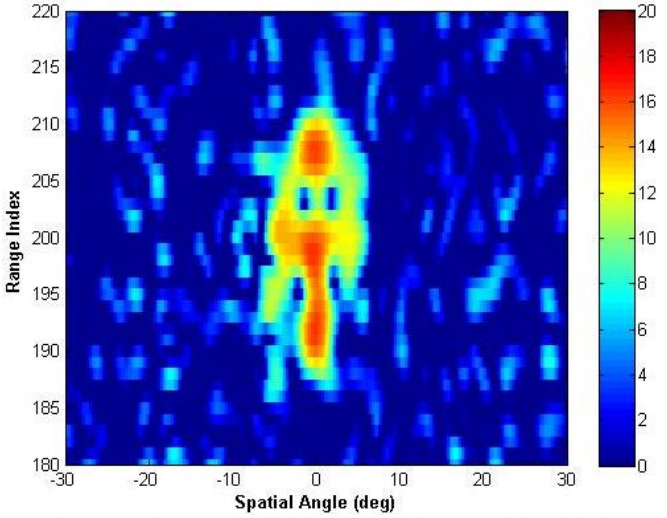

Figure 10. Five-target scenario for Case 2) linear spatial modulation

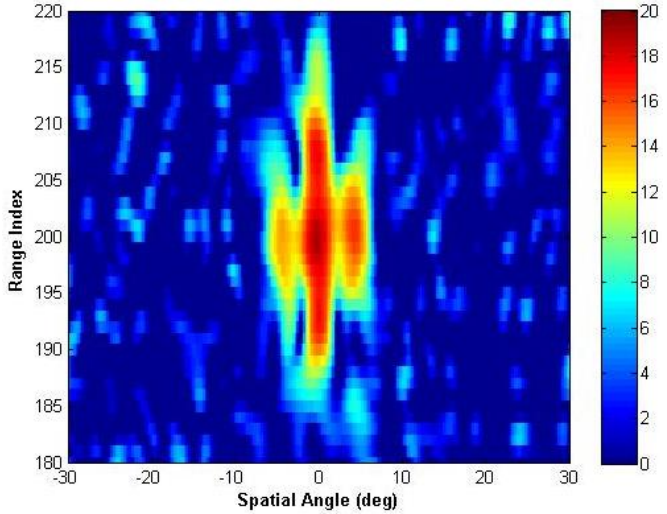

Figure 11. Five-target scenario for Case 3) double linear spatial modulation

By comparision, the two linear spatial modulation schemes (Cases 2 and 3) shown in Figs. 10 and 11 provide less definition in the range domain and SNR loss relative to Case 1, but do provide clear visualization of the angle-separated targets. Finally, the sinusoidal spatial modulation (Case 4) shown in Fig. 12 again demonstrates that it is a poor choice due to lack of resolving the angle-separated targets as well as false targets arising from high range sidelobes.

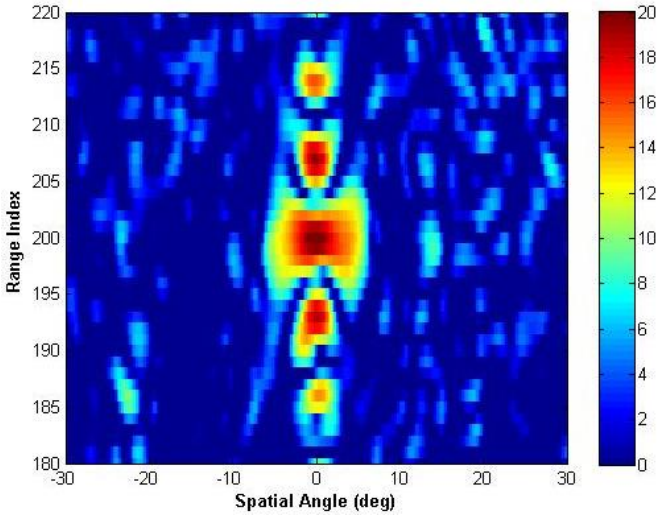

Figure 12. Five-target scenario for Case 4) sinusoidal spatial modulation

While these emission examples provide some insight into the potential of spatial modulation for enabling greater discrimination of targets in close delay/angle proximity, such as needed for the tracking application, further work is needed to ascertain the performance that may be obtained when using joint angle-delay optimized emissions via generalization of [16,17]. Along those lines, this work is also complemented by ongoing work on transmitter/waveform co-design [18] and expanded design degrees of freedom via waveform "over-coding" [19].

CONCLUSIONS

A generalization of the recently introduced continuous phase modulation (CPM) waveform implementation scheme has been introduced that enables the physical generation of spatially-modulated MIMO radar emissions. The inherent angle-delay coupling can, dependent upon the specific structure of the underlying waveform and spatial modulation codes employed, realize various trade-offs in resolution and sidelobe levels for the delay and angle domains. Further, the attendant enhanced discrimination capability on a per-pulse basis may facilitate improved tracking capability, particularly of closely-spaced targets, without the need for computationally intensive adaptive receive processing (though it is likely that doing so could provide further enhancement). By paralleling the operation of the human eye, this and subsequent related work may be able to mimic the same degree of visual acuity and discrimination and further facilitate cognitive radar capabilities.

REFERENCES

[1] J. Li and P. Stoica, *MIMO Radar Signal Processing*, Wiley-IEEE Press, 2008.

[2] D.R. Fuhrmann, J.P. Browning, and M. Rangaswamy, "Signaling strategies for the hybrid MIMO phased-array radar," *IEEE J. Selected Topics in Signal Processing*, vol. 4, no. 1, pp. 66-78, Feb. 2010.

[3] P. Antonik, M.C. Wicks, H.D. Griffiths, and C. J. Baker, "Range-dependent beamforming using element level waveform diversity," *Intl. Waveform Diversity and Design Conf.*, Lihue, HI, 22-27 Jan. 2006.

[4] T. Higgins and S.D. Blunt, "Analysis of range-angle coupled beamforming with frequency-diverse chirps," *Intl. Waveform Diversity & Design Conf.*, Orlando, FL, pp. 140-144, 8-13 Feb. 2009.

[5] P.F. Sammartino, C.J. Baker, and H.D. Griffiths, "Frequency diverse MIMO techniques for radar," *IEEE Trans. Aerospace & Electronic Systems*, vol. 49, no. 1, pp. 201-222, Jan. 2013.

[6] P.M. Corbell, M.A. Temple, T.D. Hale, W.P. Baker, and M. Rangaswamy, "Performance improvement using interpulse pattern diversity with space-time adaptive processing," *IEEE Radar Conf.*, Washington, DC, pp. 55-60, 9-12 May 2005.

[7] M.A. Richards and J.A. Scheer, *Principles of Modern Radar: Basic Principles*, SciTech, Sect. 18.9, 2010.

[8] M. Rolfs, "Microsaccades: small steps on a long way," *Vision Research*, vol. 49, pp. 2415-2441, 2009.

[9] E. Ahissar and A. Arieli, "Seeing via miniature eye movements: a dynamic hypothesis for vision," *Frontiers in Computational Neuroscience*, vol. 6, no. 89, Nov. 2012.

[10] J. Cui, M. Wilke, N.K. Logothetis, D.A. Leopold, and H. Liang, "Visibility states modulate microsaccade rate and direction," *Vision Research*, vol. 49, pp. 228-236, 2009.

[11] S. Haykin, Y. Xue, and P. Setoodeh, "Cognitive radar: step toward bridging the gap between neuroscience and engineering," *Proc. IEEE*, vol. 100, no. 11, pp. 3102-3130, Nov. 2012.

[12] S.D. Blunt, M. Cook, E. Perrins, and J. de Graaf, "CPM-based radar waveforms for efficiently bandlimiting a transmitted spectrum," *IEEE Radar Conf.*, Pasadena, CA, 4-8 May 2009.

[13] J. Jakabosky, P. Anglin, M. Cook, S.D. Blunt, and J. Stiles, "Non-linear FM waveform design using marginal Fisher's information within the CPM framework," *IEEE Radar Conf.*, Kansas City, MO, 23-27 May 2011.

[14] S.D. Blunt, M. Cook, J. Jakabosky, J. de Graaf, and E. Perrins, "Polyphase-coded FM (PCFM) waveforms: part I: implementation," to appear in *IEEE Trans. Aerospace & Electronic Systems*.

[15] H.L. Van Trees, *Optimum Array Processing*, John Wiley & Sons, 2002, Chap. 2.

[16] J. Jakabosky, S.D. Blunt, M.R. Cook, J. Stiles, and S.A. Seguin, "Transmitter-in-the-loop optimization of physical radar emissions," *IEEE Radar Conf.,* Atlanta, GA, 7-11 May 2012.

[17] S.D. Blunt, M. Cook, J. Jakabosky, J. de Graaf, and E. Perrins, "Polyphase-coded FM (PCFM) waveforms: part II: optimization," to appear in *IEEE Trans. Aerospace & Electronic Systems*.

[18] L. Ryan, J. Jakabosky, S.D. Blunt, C. Allen, and L. Cohen, "Optimizing polyphase-coded FM waveforms within a LINC transmit architecture," *IEEE Radar Conf.*, 19-23 May 2014.

[19] J. Jakabosky, S.D. Blunt, and B. Himed, "Optimization of "over-coded" radar waveforms," *IEEE Radar Conf.*, 19-23 May 2014.